

An Open-source Algorithm to Detect Onset of Arterial Blood Pressure Pulses

W Zong^{1,2}, T Heldt¹, GB Moody¹, RG Mark¹

¹Harvard University - MIT Division of Health Sciences and Technology,
Massachusetts Institute of Technology, USA

²Beth Israel Deaconess Medical Center,
Harvard Medical School, Boston, USA

Abstract

In this paper, we present an effective algorithm for detecting the onset of arterial blood pressure (ABP) pulses. The algorithm employs a windowed and weighted slope sum function (SSF) to extract ABP waveform features. Adaptive thresholding and search strategies are applied to the SSF signal to detect ABP pulses and to determine their onsets. Two evaluation procedures were employed. First, pulse detection accuracy was evaluated by comparing the algorithm's pulse detections with reference ECG annotations using the MIT-BIH Polysomnographic Database. The algorithm detected 99.31% of the 368,364 beats annotated in the ECG. Second, the accuracy of pulse onset determination was established using a newly created, manually-edited reference ABP signal database. For 96.41% of the 39,848 beats in the reference database, the difference between the manually-edited and algorithm-determined ABP pulse onset was less than or equal to 20 ms. The C source code of the algorithm has been contributed to PhysioToolkit and is freely available from the PhysioNet website (<http://www.physionet.org>).

1. Introduction

The ABP waveform contains rich information about the cardiovascular system, such as heart rate, systolic, mean, and diastolic arterial pressures, and it can be used to assess properties of the arterial vessel wall [1, 2]. Reliable and accurate ABP pulse detection is crucial for beat-by-beat extraction and analysis of the information mentioned above. This task is rendered difficult, however, since the ABP measurement is prone to noise and artifacts (see Figure 1 (b) and (d)). Furthermore, the waveform morphology can change dramatically, even over short periods of time, in response to altered pathologic or physiologic stresses (Figure 1 (a) and (c)).

Although it is the ABP pulse onset that denotes the arrival of the arterial pressure pulse at the recording site, most ABP pulse and pulse-component detection algorithms identify the peak of the ABP waveform as the fiducial

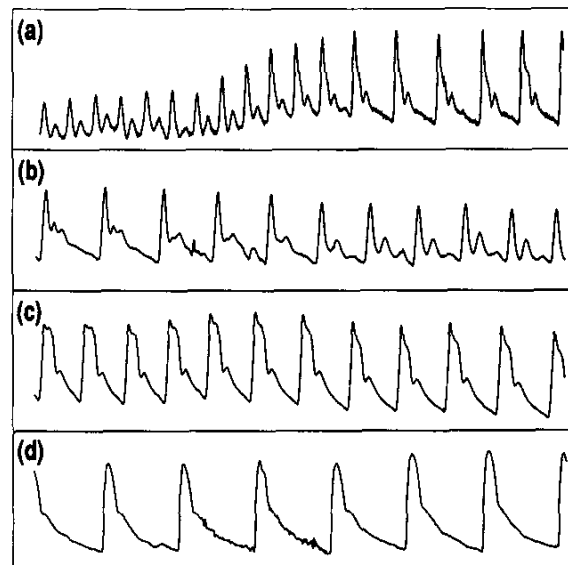


Figure 1. Examples of ABP waveform signals. (a) and (b) are non-invasive (FINAPRES) recordings; (c) and (d) are invasive ABP recordings from the radial artery; 10 seconds per trace.

mark of the ABP pulse [3, 4, 5]. The strategy of peak detection rather than pulse onset detection is inappropriate for studying pulse wave velocity [6] and ECG-ABP delay time [7] characteristics, as the duration of the upslope depends, among other things, on ventricular and valvular properties.

This study presents an algorithm that determines the onset of arterial pressure pulses by first converting the ABP waveform into a slope sum function (SSF) signal. Subsequent adaptive thresholding and local search strategies allow for ABP onset annotations to be placed in close proximity of the actual pulse onset. We used two different databases for performance evaluation. Our results show that this algorithm is effective in detecting and annotating ABP onsets.

2. Methods

2.1. The algorithm

As shown in Figure 2, the algorithm consists of three components: a low-pass filter, a windowed and weighted slope sum function, and a decision rule. The ABP signal,

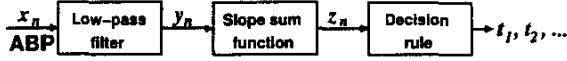


Figure 2. Algorithm flow diagram.

x_n , is the input of the low-pass filter, and y_n is the filtered ABP. The slope sum function converts y_n to a slope sum signal z_n . A decision rule is applied to z_n to determine the ABP pulse onsets denoted by t_1, t_2, \dots

Low-pass filter: The purpose of the low pass filter is to suppress high frequency noise that might affect the ABP onset detection. We use a second order recursive filter [8] whose transfer function, frequency response, and difference equation are given below for a sampling frequency of 250 Hz (i.e., a sampling interval $T = 4$ ms).

$$H(z) = \frac{(1 - z^{-5})^2}{(1 - z^{-1})^2}, \quad |H(\omega T)| = \frac{\sin^2(3\omega T)}{\sin^2(\omega T/2)}$$

$$y_n = 2y_{n-1} - y_{n-2} + x_n - 2x_{n-5} + x_{n-10}$$

The 3 dB cut-off frequency is about 16 Hz and the gain is 25 at 0 Hz. The phase shift is 20 ms (5 samples at 250 Hz).

Slope sum function: The purpose of the slope sum function is to enhance the upslope of the ABP pulse and to suppress the remainder of the pressure waveform. The windowed and weighted slope sum function at time i , z_i , is defined as follows:

$$z_i = \sum_{k=i-w}^i \Delta u_k, \quad \Delta u_k = \begin{cases} \Delta y_k & : \Delta y_k > 0 \\ 0 & : \Delta y_k \leq 0 \end{cases}$$

where w is the length of the analyzing window; $1 + w \leq i \leq N$, N is the total number of ABP samples in the record; $\Delta y_k = y_k - y_{k-1}$, and y_k is the low-pass filtered ABP signal as defined above. To maximize the SSF, w is chosen approximately equal to the typical duration of the upslope of the ABP pulse. In the present algorithm, $w = 128$ ms or 32 samples for the sampling frequency of 250 Hz. The relationship between the ABP and the SSF signals is shown in Figure 3.

The onset of the SSF pulse generally coincides with the onset of the ABP pulse as the SSF signal can only rise when the ABP signal (or noise not removed by filtering) rises.

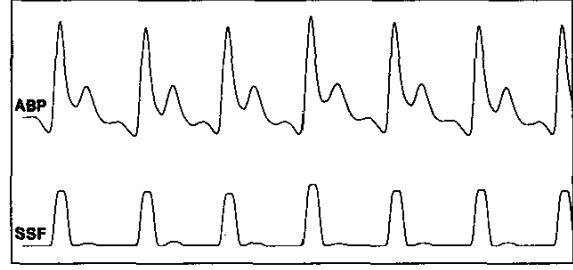


Figure 3. Relationship between ABP and SSF signals.

Since the SSF signal is a simpler signal to process, the pulse onset will be detected by processing the SSF signal.

Decision rule: Finally, we have to establish a decision rule that allows for detection of each SSF pulse onset. We split this task into two: First, we apply adaptive thresholding to the SSF signal to detect SSF pulses of appropriate amplitude. Next, we employ a local search strategy around the detection point to confirm the detection and to identify the likely onset of the pulse. During the thresholding step, a threshold base value is established and is initialized at three times the mean SSF signal (averaged over the first ten seconds of the recording). The threshold base value is adaptively updated by the maximum SSF value for each SSF pulse detected. The actual threshold is taken to be 60% of the threshold base value. When the SSF signal crosses this threshold, the algorithm searches for the minimum and the maximum SSF values in a 150 ms-window preceding and succeeding the threshold-crossing point, respectively. The pulse detection is accepted only if the difference between the maximum and minimum exceeds a certain value; otherwise the pulse detection is rejected. When the pulse is accepted, the algorithm searches backward in time from the threshold-crossing point for the onset of the SSF pulse. The onset point is determined when the SSF signal exceeds 1.0% of the maximum SSF value. The calculated ABP onset is adjusted by 20 ms, or 5 samples, to compensate for the low-pass filter's phase shift. Finally, to avoid double detection of the same pulse, a 300ms eye-closing (refractory) period is applied, during which no new pulse detection is initiated. Figure 4 illustrates the ABP onset annotations.

2.2. Evaluation procedure

To evaluate the performance of the algorithm, we first assessed the accuracy of pulse detection and subsequently evaluated the accuracy of pulse onset detection.

Pulse detection: The pulse detection accuracy of the algorithm was evaluated using the MIT-BIH Polysomno-

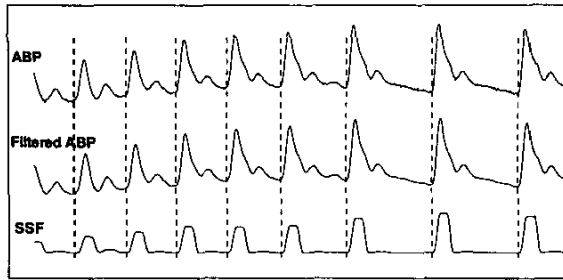


Figure 4. Example of ABP pulse onset detection process. Top trace: raw ABP signal; middle trace: filtered ABP signal; bottom trace: SSF signal; vertical dashed lines: ABP onset annotations.

graphic Database [9, 10], which consists of 18 recordings of variable length, each of which contains, among other physiologic signals, an invasively recorded ABP signal. Given a relatively constant delay between the QRS complex and peripherally recorded ABP signals of about 200 ms, we compared the ABP pulse detections with the reference ECG-based beat annotations by shifting forward the ECG annotations by 200 ms and applying a standard beat annotation comparison, bxb [11], freely available from PhysioNet. A total of 368,364 ECG-based beat annotations are available for comparison.

Pulse onset detection: To assess the accuracy of the pulse onset detection, a reference database was established, which includes ten one-hour recordings of ECG and a non-invasively measured ABP signal (FINAPRES). The details of the database are described elsewhere in these proceedings [12]. In a first step, we used the algorithm above to annotate the ABP pulses. In the second step, a human expert annotator carefully inspected each ABP onset detection and, where deemed necessary, manually edited the annotation placement. A comparison between the location of the manually-edited and algorithm-based annotations was then performed using bxb, which allows for specification of a match window, i.e., a maximum absolute difference in annotation times permitted for matching annotations. Only if two annotation times deviate by less than the user-specified matching window, is a correct annotation declared. A total of 39,848 ABP annotations are available in the reference database for comparison. This number includes 560 annotated blood pressure calibration pulses.

3. Results

A high level of concurrence was observed for the evaluation of pulse detection using the MIT-BIH

Polysomnographic Database: 99.31% of the 368,364 beats annotated in the ECG were detected by the algorithm, and 99.74 % of the events detected by the algorithm had been annotated as beats in the ECG. Many of the discrepancies occur as a result of ECG or ABP signal loss. Table 1 shows the summary statistics for the pulse detection evaluation.

Table 1. Sensitivity and PPA of pulse detection I

	Sen (%)	PPA (%)
Gross	99.31	99.74
Average	99.26	99.77

PPA: positive predictive accuracy.

Similar results were obtained when evaluating the performance of pulse detection on the reference database described above: 99.71 % of the 39,848 reference ABP annotations were detected by the algorithm, and 99.69 % of the events detected by the algorithm were in fact annotated ABP pulses. Table 2 reports the summary statistics for pulse detection using the newly established reference database.

Table 2. Sensitivity and PPA of pulse detection II

	Sen (%)	PPA (%)
Gross	99.71	99.69
Average	99.71	99.72

We also used the reference database described above to assess the accuracy of the ABP pulse onset determination. Figures 5 and 6 show the histogram and cumulative distribution of matching annotations as a function of Δt , the time difference between the manually and algorithmically determined ABP pulse onsets. As can be seen, most annotations fall within 8 ms of the reference annotations, with outliers tapering off gradually.

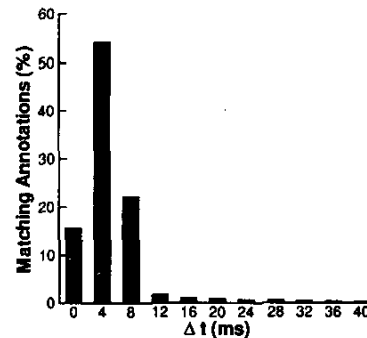


Figure 5. Histogram of matching annotations as a function of Δt .

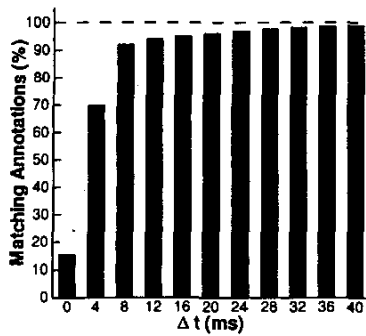


Figure 6. Cumulative distribution of matching annotations as a function of Δt .

For 96.41% of the 39,848 beats in the reference database, the difference between the manually-edited and algorithm-determined ABP pulse onset was less than or equal to 20 ms.

4. Discussion

Accurate detection of arterial blood pressure pulse onsets enables one to extract physiologic information from arterial pressure waveforms on a beat-by-beat basis.

Our approach to ABP pulse onset detection is based on the transformation of a low-pass filtered ABP signal into a slope sum function signal, in which the initial upslope of the blood pressure waveform is enhanced and the remainder is suppressed. The transformation leaves the location of the pulse onset unaltered, except for the fixed filter delay, and detection of the pulse onset based on the slope sum function signal is straight forward.

Our evaluation results indicate that the vast majority of algorithm-based blood pressure pulse onset annotations are placed within a few samples' distance from annotations placed by an expert annotator.

Finally, we have included the algorithm in the open-source WFDB software package, which is freely available from PhysioNet (<http://www.physionet.org/>)

Acknowledgments

This work was supported in part by the Research Resource for Complex Physiologic Signals, NIH/NCRR, Grant P41 RR 13622, and by NASA through the NASA Cooperative Agreement NCC 9-58 with the National Space Biomedical Research Institute.

References

- [1] O'Rourke MF, Kelly RP, Avolio, AP. The arterial pulse. Lea & Febiger, Malvern, PA, 1992.
- [2] Miyakawa K, Koepchen HP, Polosa C. Mechanisms of blood pressure wave. Japan Scientific Societies Press, Springer-Verlag, Tokyo, 1984.
- [3] Antonelli L, Khanmlach R. Wavelet transform analysis of the arterial pressure waveform. Computers in Cardiology 1994:568-571.
- [4] Aboy M, et al. Automatic detection algorithm for physiologic pressure signal components. Proc 2nd Joint EMBS/BMES Conference 2002:196-197.
- [5] Navakatiyan MA, et al. A real-time algorithm for the quantification of blood pressure waveforms. IEEE Trans. Biomed. Eng. 2002; 49(7):662-670.
- [6] Lehmann ED, D. HK, Golsling RG. Assessment of arterial distensibility by automatic pulse wave velocity measurement. Hypertension 1996; 27(5):1188-1191.
- [7] Zong W, Moody GB, Mark RG. Effects of vasoactive drugs on the relationship between ECG-pulse wave delay time and arterial blood pressure in ICU patients. Computers in Cardiology 1998; 25:673-676.
- [8] Lynn PA. Online digital filter for biological signals: some fast designs for a small computer. Med Biol Eng Comput 1977; 15:534-540.
- [9] Ichimaru Y, Moody GB. Development of the polysomnographic database on CD-ROM. Psychiatry and Clinical Neurosciences 1999; 53:175-177.
- [10] Goldberger AL, et al. PhysioBank, PhysioToolkit, and PhysioNet: components of a new research resource for complex physiologic signals. Circulation 2000; 101(23):e215-e220.
- [11] Moody GB. Evaluating ECG analyzers. In: *WFDB Applications Guide*. Freely available from <http://www.physionet.org>.
- [12] Heldt T, et al. Circulatory response to passive and active changes in posture. Computers in Cardiology 2003; 30.

Address for correspondence:

Wei Zong, PhD
Massachusetts Institute of Technology
Room E25-505
77 Massachusetts Avenue
Cambridge, MA 02139, USA
wzong@mit.edu